Open Access Journal

Journal of Power Technologies 98 (1) (2018) 127–138

journal homepage:papers.itc.pw.edu.pl

The New Adaptive Under Frequency Load Shedding Technique in an Automated Distribution Network Considering Demand Response Programs

Amin Mokari-Bolhasan, Navid Taghizadegan-Kalantari*

Electrical Engineering Department, Faculty of Engineering, Azarbaijan Shahid Madani University, Tabriz, Iran

Abstract

Under Frequency Load Shedding (UFLS) is an important protection scheme to maintain the frequency of a Distribution Network (DN) consisting of Distributed Generations (DGs) exposed to power deficit. The different location and amount of load curtailments based on different parameters are acquired from the available literature. In this paper, an optimal adaptive UFLS method with the advent of two main modules has been proposed. The proposed method provides a revised Rate of Change of Load (ROCOFL) index related to bus voltage and load power consumption ($ROCOFL_{pv}$). Using a wide area measurement system, Demand Response (DR) technology aimed at shedding fewer loads is emerging against a background of the smart grid. In addition, smart appliances can provide a real-time data packet in which frequency, the rate of change of frequency, voltage magnitude and breaker status are measured. The proposed method is implemented in five different load schemes considering DR programs. Comparative analyses are illustrated in this paper to assert the efficiency of implementing DR programs in which cost function and amounts of shedding loads are decreased. The results demonstrate that DR programs cannot be used for a big power unbalance in an islanded micro grid. The unintentional delay time imposed by DR and the small inertia existing in an islanded distribution network restrict the use of DR programs.

Keywords: Under Frequency Load shedding; Rate of Change of Frequency of Load; Distributed Network Operator; Smart-Grid; Distribution Management System; Demand Response

1. Introduction

Frequency stability is a huge issue during the evolution of outages [22, 27]. The system can lose balance through an increment of load or a failure in the power supply. When there is a major deviation between consumption and generation, UFLS methods are used. UFLS methods are categorized as traditional, semi-adaptive and adaptive techniques [6]. Adaptive UFLS procedures can be modified, with the advent of centralized UFLS schemes and power system automation to shed appropriate amounts of loads [8, 28, 29].

The Rate of Change of Frequency (ROCOF) and power swing equation can be used to provide an estimation of the power deficit in an adaptive UFLS method. If the frequency of the system has been decreased to a specified amount, the UFLS method will be activated. Using a calculated primary ROCOF, the amounts of shedding loads are determined [21, 26]. In Anderson and Mirheydar [1], a System Frequency Response (SFR) flowchart and proposed reduced models are proposed, which can facilitate the procedure for calculating the power deficit. Power system load is influenced by variations in voltage. A major drawback of using the SFR model is that load voltage dependency is not factored in. Some researchers have factored in load voltage dependency when calculating unbalanced power [11, 17, 19]. An adaptive SFR model incorporating system inertia, response of governors, load frequency and voltage dependence is presented in [23]. According to [13], the calculated primary ROCOF should be multiplied by a specified factor to consider load voltage dependency. Uncertainty is the major drawback of distant adaptive UFLS methods in determining power deficit.

In [10], the author presents a centralized adaptive UFLS controller (CAULSC) that makes use of frequency, ROCOF and a distribution state estimator (DSE) when estimating load demand to maintain system frequency response. In contrast to most adaptive schemes, the author in [20] solves the problem of power deficit estimation in which system voltage variation during an islanding mode is considered. In this method, the future minimum frequency value – determined by implementing the frequency versus Frequency First Time

*Corresponding author

Email address: taghizadegan@azaruniv.edu (Navid Taghizadegan-Kalantari)

Derivative (FTD) phase-plane – can be predicted for various scenarios.

The priority and locality of the loads to be curtailed is of great importance in the load shedding procedure. ROCOFL indices presented in [12] provide a correct comparison and selection of loads to shed sufficiently. An optimal load shedding method which uses an optimization solution to create a load priority look-up table is presented in [14]. The interruption cost of dropped loads is dealt with in [7] as part of an economical load shedding process. Three stages are proposed in [7] that can be divided into the following categories:

- Requirement Analysis (RA),
- Pre-disturbance Preparation (PP),
- Real-Time (RT).

The CPLEX solution pool feature provides an optimal cost effective solution to solve the load shedding problem [7]. Reddy et al. [18] carried out a phasor measurement unit (PMU) sensitivity study to determine the location and size of loads to be shed. In [24] representative Operating and Contingency (OC) schemes are selected. The UFLS scheme can be rendered more efficient by applying an optimization algorithm such as Simulated Annealing (SA) to adjust the UFLS scheme parameters, as in [24]. Step sizes are not factored in as decision variables and only frequency, ROCOF thresholds and internal time delays are optimized. [25] proposes finding the optimal load shedding while satisfying the load flow equation and having static power system constraints such as line flows, voltages, angular limits and shedding constraints. A hybrid technique combining the Genetic Algorithm (GA) and Artificial Neural Network (ANN) is implemented in [25] to minimize load shedding and voltage deviation. Smart grid approaches for UFLS procedures are fully explained in [5, 15].

Increasing attention is being paid to Demand Response (DR) programs to control frequency of the system, using economic incentives to maintain frequency responses. Many DR frequency control strategies are presented involving disturbance magnitude estimation based methods, hill climbing control methods and methods based on Linear Quadratic Regulator (LQR) for controlling frequency of singular areas. In [30] the author presented a DR control methodology which uses tie-line power swing as a conventional feedback control signal in a multi-area system. This method makes use of a multi-objective optimization problem to optimally determine parameters of DR and AGC control. Loads can be divided into controllable and non-controllable loads. Loads used in DR programs are usually considered non-essential loads. For instance, these loads include heating, ventilation and air conditioning (HVAC) systems, water heaters, refrigerators and so forth. Increasing or decreasing these residential loads would not affect their convenience. According to [4] DR appliances consist of electrical appliances and controllers. Controllers can manage electrical appliances by changing the convenient set point.

In [3] the author applies the DR program to the area after calculating the magnitude of unbalance and determining the area in which a disturbance has occurred. A regional DR tasked with cooperating in system frequency control of multi-area power systems is also presented in [2]. This method makes use of the second derivative of tie-line power to extract the size and location of disturbances during contingent events.

Modern distribution networks will be equipped with Information and Communication Technology (ICT), in light of advances in smart grid systems [16]. In [31] a real time control approach is illustrated. Load curtailments are assumed as part of DR programs to keep the distribution feeder voltage within a specified range. In this methodology an emergency demand response program is used in the proposed real time voltage control model to counteract DG outage or renewable generation and load demand unpredictability. In this paper, a Supervisory Control and Data Acquisition (SCADA) solution brings with it comprehensive merits for monitoring and controlling tasks in Distribution Automation (DA) and Distribution Management System (DMS).

In the current paper a new optimal UFLS scheme for islanded distribution system integrated with DGs is proposed. Here, it is not necessary to use the reduced SFR pattern to estimate the power deficit. Moreover, the proposed procedure offers a ROCOF based method that assumes load voltage dependence and network critical frequency. Regardless of the previous methods, this paper factors in load voltage and frequency dependence during the ROCOFL determination. The revised ROCOFL*pv is presented in this paper and involves voltage dependence of loads with a view to shedding fewer – and more accurate – amounts of loads. In this paper, an optimal adaptive UFLS method with two main modules is proposed. The two main modules presented in this paper are: Pre-determined Load Shedding Calculator (PLSC) and Determined Load Shedding Calculator (DLSC). These two main modules provide an accurate load shedding procedure. This paper also reports on the effect of DR programs in an islanded distribution network. The emergency demand response program (EDR) provides consumers with a lower electricity price, since they are supposed to cut their consumption when the system faces an unbalance. The Distribution Network Operator (DNO) encounters fewer shedding loads and a cost function reduction when DR programs are implemented. DR programs also impose an excessive unintentional delay time, which can cause a limitation boundary on use of these methods. For large power unbalances, system frequency experiences an unallowable minimum frequency threshold which leads to a network blackout. In this paper, the General Algebraic Modeling System (GAMS) is used to develop an optimal load shedding procedure. Comparative simulations based on different load schemes are also analyzed in Digsilent Power Factory software to prove this theory.

This paper is organized as follows: In section 2, the proposed algorithm is presented. In section 3, the test system is explained. In section 4, the proposed method is implemented on a Danish 14 bus test case. In section 5, results are proposed.

2. Proposed Load Shedding Method

With a view to preventing system collapse, periodical and real-time data are continuously sent to inform mandatory activities and choose the best loads to optimize the load shedding procedure. The network will return to its nominal frequency and an islanded grid can sustain its usual process through the micro-grid by curtailing pre-determined loads.

At this point, the index of ROCOFL is proposed for every load using the method presented as follows. In this method, firstly, we create an islanded network with existing elements. To determine the ROCOFL index, the amount of load must be duplicated at the bus intentionally. Initial ROCOF is measured to determine the ROCOFL index related to the load. In [13] loads are supposed to be constant when calculating the ROCOFL, which can cause over shedding. In this paper, loads are considered voltage and frequency dependent during determination of the ROCOFL index. In this paper the $ROCOFL_{pv}$ index is proposed to create a loads look-up table for the shedding procedure. In addition, system centralized frequency and ROCOF are calculated by Eqs. (1) and (2) respectively, in the case of islanding [14].

$$f_c = \frac{\left(\sum_{n=1}^{m} f_n \times H_n\right)}{H_C} \tag{1}$$

$$ROCOF_C = \frac{\left(\sum_{n=1}^{m} ROCOF_n \times H_n\right)}{H_C} \tag{2}$$

In this paper, an optimal adaptive UFLS method with two main modules is proposed. These modules are presented below.

2.1. PLSC module

The algorithm used in this module is depicted in Fig. 1. In this algorithm, generator frequency and rate of change of frequency are sent every half cycle to the DMS by Remote Terminal Units (RTUs). Since the status of the generator's breakers is important for the calculation of system central inertia, this status is also received by DMS every half cycle. To update ROCOFL indices, load power consumption must be sent periodically to the control center. Here, loads are considered dynamic, dependent on system frequency and voltage. Centralized frequency and ROCOF are calculated when the system is going to enter islanded mode unintentionally. $ROCOFL_{pv}$ index is a value that can be updated using Eq. (3).

$$ROCOFL_{pv}^{*} = ROCOFL \times \left(\frac{P_i^L}{P_0}\right) \times \left(\frac{V_i{}^L}{V_0}\right)^{K_{pv}} \tag{3}$$

To obtain pre-determined loads for implementing the load shedding procedure, the minimizing procedure for the cost function problem using Eq. (4) is used, which factors in the calculated $ROCOFL_{pv}^{*}$.

The periodically updated $ROCOFL_{pv}^{*}$ shows the load ROCOF index related to active power and voltage. P_0 and V_0 are the nominal power and voltage respectively. In addition, P_i^L and V_i^L are active power and voltage of ith bus related to load L. K_{pv} shows the relativity of load active power to voltage. In this paper, loads are voltage and frequency dependent. The model for the loads is the same as one presented in Mohammadi-Ivatloo et al. [13]. The presented UFLS method depends on the amounts and location of shedding loads. The UFLS problem is formulated as a cost function using Eq. (4).

$$\min \; f(x) = \sum_{s=1}^{P} E(C_{LS,s}^{t}) P_{LS,s}(x) \tag{4}$$

The cost of load shedding imposed by a particular event is achieved through using Eq. (5). It is obtained by multiplying the Expected Energy not Supplied (EENS) in brownout interval of t for the sth load combination scheme and a coefficient called the Value of Lost Load (VOLL).

$$E(C_{LS,s}^{t}) = VOLL \times EENS_{s}^{t} \tag{5}$$

VOLL is the estimated amount that customers receiving electricity with firm contracts would be willing to pay to avoid disruption to their electricity service. Constraints can be categorized in two parts. The first part relates to the power system and the second part relates to the performance of the UFLS scheme. The constraints of the first part are as follows:

- The power flow equations must be satisfied in each substation.
- The voltage of each bus and its angle should be kept within safe operating limits.
- Power limits of every substation should be fulfilled.
- Power limits of generation units must be satisfied.
- Line thermal restrictions between substations must be satisfied.

The constraints of the second part related to UFLS scheme are presented as follows:

- For the purpose of avoiding insufficient curtailment, we must calculate the difference between initial centralized ROCOF ($ROCOF_{C0}$) and critical ROCOF ($ROCOF_{Cr}$). Therefore revised centralized ROCOF ($ROCOF_{C0}$) can be determined Using Eq. (6).
- Using Eq. (7), ROCOF constraint should be satisfied. According to this constraint, the sum of the updated $ROCOFL_{pv}$ should be bigger than the revised measured primary ROCOF.

$$ROCOF_{C0}^{*} = ROCOF_{C0} - ROCOF_{Cr} \tag{6}$$

$$\sum_{s=1}^{p} ROCOFL_{pv,s}^{*}(x) > ROCOF_{C0}^{*} \quad (7)$$

In accordance with the presumed cost function and limitations, DMS implements the proposed algorithm. So, DMS can determine pre-determined loads by factoring in the expected costs of shedding loads.

2.2. DLSC module

Pre-determined loads provided by PLSC are sent to this module to determine loads that should be curtailed to bring the system to the normal state. In this module, the proposed algorithm is illustrated in Fig. 2.

In this algorithm, time delays and frequency threshold values for the first step are T_1 and f_{T1}. When an obtained $ROCOF_{C0}$ value is greater than $ROCOF_{Cr}$, this algorithm goes through the first curtailment step. In this step, when f_C is less than f_{T1} for T_1 seconds, y_1 (percent) of pre-determined loads are being curtailed. After the first step, if f_C is less than f_{T2} for T_2 seconds, $y_2 \cdot (1 - y_1)$ (percent) of pre-determined loads will be curtailed. When f_C is less than f_{T2} for T_2 seconds, directly, the second step curtails both first and second step loads $(y_1 + y_2)$ (percent) totally. Finally, all of the pre-determined loads are curtailed when f_C is less than f_{T3}. All of the loads are shed provided that the calculated $ROCOF_{C0}$ value is greater than $ROCOF_T$.

$ROCOF_T$ threshold value obtained through the study of different scenarios. It is determined for the case where 30 percent of generation is lost [14]. According to the operation of circuit breakers, we assume a specified imposed delay time for the shedding procedure. By means of the suggested procedure, the UFLS pattern is able to work as well as returning the system to its normal operation safely and economically.

3. Case Study

To arbitrate the performance of proposed algorithm, a set of load schemes are simulated in the Danish 14 bus test case. The detailed description and related data of this network is given in Mahat et al. [12]. The test case contains three fix-speed Wind Turbine Generators (WTGs) separately rated at a capacity of 630 kW and a Combined Heat and Power (CHP) plant with three gas turbine generators separately rated at a capacity of 3 MW. The test system illustrated in Fig. 3 is modeled using Digsilent Power Factory and GAMS technologies. To appraise the performance of the first proposed module, GAMS technology is used. Pre-determined loads are achieved optimally by optimizing the cost function problem using GAMS solution pool features. In order to analyze the performance of the second proposed module, Digsilent Power Factory software is used. The typical model utilized for CHP component is depicted in [9].

The distribution network consists of ten buses and eleven loads. In this paper, we consider in approximate terms fifteen percent of the loads in each bus as smart loads. These loads can participate in EDR programs automatically by receiving DR signal from DMS. On the other hand, eighty-five percent of loads are not flexible loads, so they cannot participate in EDR programs. In the shedding procedure, DR loads are curtailed firstly to compensate an emergency unbalance. All in all, loads are presumed to be voltage and frequency dependent in both considered states.

Table 1: Load data for the Danish 14-bus network [13]

Load	P, MW	Q, MW	P, MW	Load	Q, MW)
L_1	0.0977	0.02847	L1-DR	0.01725	0.0050
L_2	0.0977	0.02847	L2-DR	0.01725	0.0050
L_3	0.0977	0.02847	L3-DR	0.01725	0.0050
L_4	0.6156	0.1796	L4-DR	0.1086	0.0317
L_5	0.3908	0.1139	L5-DR	0.0689	0.0201
L_6	1.7926	0.4896	L6-DR	0.3163	0.0864
L_7	0.9962	0.1181	L7-DR	0.1758	0.0208
L_8	2.3222	0.7157	L8-DR	0.4098	0.1263
L_9	1.6847	0.1895	L9-DR	0.2973	0.0334
L_{10}	1.4076	0.3264	L10-DR	0.2484	0.0576
L_{11}	0.765	0.1394	L11-DR	0.135	0.0246

Load active and reactive power dependence is modeled using Eqs. (8) and (9) [14].

$$P_i^L = P_0 \left(\frac{V_i^L}{V_0} \right)^{K_{pv}} \left(1 + K_{pf} \times \frac{\Delta f}{f_0} \right) \quad (8)$$

$$Q_i^L = Q_0 \left(\frac{V_i^L}{V_0} \right)^{K_{qv}} \left(1 + K_{qf} \times \frac{\Delta f}{f_0} \right) \quad (9)$$

Where K_{pv}, K_{qv} parameters outline the dependence of active and reactive powers on voltage amount, and set to 1 and 2 individually. On the other hand, K_{pf}, and K_{qf} parameters define the dependence of active and reactive powers on frequency, and set to 1 and –1.

The power consumption of each load is illustrated in Table 1. The distribution network will continue to work as an islanded system further to a problematic brownout. All the parameters used to model generator exciters and governors are set out in the appendix.

4. Simulation Results

All the simulation outcomes are obtained by DigSilent Power Factory. Here, we look at two types of controllable and non-controllable loads. Conventional loads are not controllable, while smart loads are controllable and can be used in demand response programs in an islanded distributed network.

In this paper, five different load schemes are considered, as follows:

First scheme: Considering existing load amounts without generators brownouts in an islanded micro-grid.

Second scheme: Considering existing load amounts with WTGs brownouts in an islanded micro-grid.

Third scheme: L_1, L_2, L_3, L_4, L_7, L_9, and L_{10} are 10 percent raised without generator brownouts in an islanded micro-grid.

Fourth scheme: Loads are 10 percent raised without generator brownouts in an islanded micro-grid.

Fifth scheme: Loads are 10 percent raised with WTGs brownouts in an islanded micro-grid.

For each load, the suggested method needs the ROCOFL index to be calculated. ROCOFL index values are reliant on the grid load and inertia amounts. According to Eq. (3), the proposed $ROCOFL^{*}_{pv}$ index related to load active power and voltage can be achieved. Proposed $ROCOFL^{*}_{pv}$ values obtained from load amounts are presented in Table 2. Here, an optimal UFLS procedure is applied regarding the VOLL of each load illustrated in Table 3.

The VOLL of each load is obtained by performing an energy market analysis dependent on established cost functions and system limitations for every load scheme. By multiplying the marginal cost of each conventional and smart loads to 100 and 10 respectively, the VOLL value of each load can be determined. The frequency thresholds of f_{T1}, f_{T2}, and f_{T3} are 49, 48.5, and 48 respectively. The deliberate delay times of T_1, T_2 are 100, 200 individually. The deliberate delay time imposed by the operation of the elements and communication system is estimated 100 ms if we use demand response programs and 80 ms provided that DR programs are not used. In this proposed methodology, y_1 and y_2 are presumed step sizes, where each of them is considered 50 percent. Generator output powers are listed for different considered load schemes in Table 4.

The distribution network is disconnected from the subtransmission grid at time t=2 second (s). Fig. 4 displays the network frequency through an islanding operation without a load shedding implication in five various load schemes. The simulation results show the network frequency is not stable. The frequency is not able to reach the suitable extent of frequency within 10 second(s). Generators under frequency relays will activate and network blackout will happen if the UFLS procedure does not operate well.

Pre-determined loads and amounts of cost function (f(x)) in each load scheme obtained by the PLSC module are shown in Table 5.

According to the type of load scheme, curtailing loads can be achieved using the second proposed module (DLSC module). The suggested UFLS procedure employed in various load schemes is illustrated in Table 6. This Table presents the minimum acceptable frequency occurring in the network. In the first load scheme, $L_{3\text{-}DR}$, $L_{6\text{-}DR}$ and $L_{8\text{-}DR}$ are not shed, whereas they are chosen to be shed in the first module. The results show that the suggested UFLS scheme restores system frequency to the normal state after 10 second (s). Fig. 5 presents the CHP frequency after curtailing loads in various load schemes using the proposed UFLS procedure.

Generators begin to malfunction at a frequency of 47.5 Hz. It is necessary to avoid the frequency falling below 47.5 Hz. In this paper, the frequency for all of the load schemes after the load shedding process reaches the minimum acceptable frequency.

According to the simulations, system frequency encounters a malfunction if the amount of the power deficit is increased. Here, because of the unintentional delay time imposed by the DR programs at issue and the small amount of islanded network inertia, the system is vulnerable to large amounts of power deficit.

By and large, to comparatively analyze the efficiency of the proposed method we implemented this method in the system without using DR programs. After implementation of the load shedding procedure, the frequency response results are illustrated in Fig. 6.

Since the considered unintentional delay time is smaller than the one where DR is implemented, the system frequency response is very much more acceptable here. In order to analyze the effect of DR in an islanded network, we note the imposed cost that DNO supposed to pay to the loads that are being shed.

In Fig. 7, the cost function in the islanded network is compared in two different considered states (with and without DR program). The cost function is dramatically decreased when we use DR programs in our proposed load shedding procedure. In other words, using DR programs can save approximately US$ 20,000 per hour in terms of shedding determined loads. The amounts of curtailing loads for both states are shown in Fig. 8.

All in all, the amounts of shedding loads are smaller when DR programs are used, since they provide abundant choices of shedding loads and a large selection pool.

Regarding the outcomes, in a distribution system, not all of the pre-determined loads need to be curtailed. Using the proposed method, loads in each step are shed to reach frequency thresholds.

In this section, the proposed load scheme is simulated in the determined study case. It is clear that the suggested UFLS procedure can curtail optimal loads. Although DR programs impose an excessive unintentional delay time, they can be efficient in terms of reducing the cost function and through providing convenience.

5. Conclusions

This paper introduces a new optimal UFLS scheme for islanded distribution systems integrated with DGs. This algorithm makes use of ROCOFL indices to create a loads lookup table for shedding. In this paper, loads are considered as voltage and frequency dependent during ROCOFL determination, in spite of loads previously being viewed as fixed in similar cases in the literatures. The revised $ROCOFL^{*}_{pv}$ presented in this paper considers the voltage dependence of loads during islanding. This adaptive UFLS scheme sheds loads by measuring the primary ROCOF of the system and minimizes DNO costs imposed by VOLL. In this adaptive method, frequency thresholds, size of shedding loads and delay times in each step are changed by the severity of the event. In this paper, an optimal adaptive UFLS method with the advent of two main modules is proposed. These two modules provide an accurate load shedding procedure. In this paper, the estimation of the power deficit by reduced

Table 2: $ROCOFL^{*}_{pv}$ amounts

Load	First scheme	Second scheme	Third scheme	Fourth scheme	Fifth scheme
L_1	-0.3825	-0.3782	-0.425	-0.4165	-0.408
L_{1-DR}	-0.0675	-0.0667	-0.075	-0.0735	-0.072
L_2	-0.3825	-0.3782	-0.425	-0.4165	-0.408
L_{2-DR}	-0.0675	-0.0667	-0.075	-0.0735	-0.072
L_3	-0.3825	-0.3782	-0.425	-0.4165	-0.408
L_{3-DR}	-0.0675	-0.0667	-0.075	-0.0735	-0.072
L_4	-2.5075	-2.4225	-2.754	-2.72	-2.652
L_{4-DR}	-0.4425	-0.4275	-0.486	-0.48	-0.468
L_5	-1.5725	-1.53	-1.5725	-1.717	-1.67
L_{5-DR}	-0.2775	-0.27	-0.2775	-0.303	-0.2955
L_6	-7.35	-7.225	-7.361	-7.9815	-7.8
L_{6-DR}	-1.2975	-1.275	-1.299	-1.4085	-1.377
L_7	-4.0375	-3.9525	-4.4455	-4.386	-4.2925
L_{7-DR}	-0.7125	-0.6975	-0.7845	0.774	-0.7575
L_8	-9.6475	-9.435	-9.605	-10.446	-10.208
L_{8-DR}	-1.7025	-1.665	-1.695	-1.8435	-1.801
L_9	-6.9275	-6.8	-7.6245	-7.5225	-7.3525
L_{9-DR}	-1.2225	-1.2	-1.695	-1.8435	-1.2975
L_{10}	-5.7375	-5.61	-6.3155	-6.2305	-6.086
L_{10-DR}	-1.0125	-0.99	-1.1145	-1.0995	-1.074
L_{11}	-3.0855	-3.0175	-3.077	-3.3405	-3.264
L_{11-DR}	-0.5445	-0.5325	-0.543	-0.5895	-0.576

Table 3: VOLL values in different load schemes

Load	First scheme	Second scheme	Third scheme	Fourth scheme	Fifth scheme
L_1	12011.3	12048.3	12015.6	12016.3	12053.4
L_{1-DR}	1201.13	1204.83	1201.56	1201.63	1205.34
L_2	12023.4	12038	12026.8	12027.4	12042
L_{2-DR}	1202.34	1203.8	1202.68	1202.74	1204.2
L_3	12023.5	12036.1	12026.8	12023.7	12039.9
L_{3-DR}	1202.35	1203.61	1202.68	1202.37	1203.99
L_4	12020.7	12025.8	12022.9	12023.5	12028.5
L_{4-DR}	1202.07	1202.58	1202.29	1202.35	1202.85
L_5	12011.1	12013.3	12012.1	12012.6	12014.8
L_{5-DR}	1201.11	1201.33	1201.21	1201.26	1201.48
L_6	12000.6	12000.6	12000.7	12000.8	12000.8
L_{6-DR}	1200.06	1200.06	1200.07	1200.08	1200.08
L_7	12000.6	12000.6	12000.7	12000.8	12000.8
L_{7-DR}	1200.06	1200.06	1200.07	1200.08	1200.08
L_8	12000.6	12000.6	12000.7	12000.8	12000.8
L_{8-DR}	1200.06	1200.06	1200.07	1200.08	1200.08
L_9	12000.6	12000.6	12000.7	12000.8	12000.8
L_{9-DR}	1200.06	1200.06	1200.07	1200.08	1200.08
L_{10}	12000.6	12000.6	12000.7	12000.8	12000.8
L_{10-DR}	1200.06	1200.06	1200.07	1200.08	1200.08
L_{11}	12000.6	12000.6	12000.7	12000.8	12000.8
L_{11-DR}	1200.06	1200.06	1200.07	1200.08	1200.08

Table 4: Generators active power in various load schemes

Generator	First scheme	Second scheme	Third scheme	Fourth scheme	Fifth scheme
$P_{Sub-Trans}$, MW	2.91	3.16	3.498	4.118	4.369
P_{CHP}, MW	9	9	9	9	9
P_{W1}, MW	0.084	0	0.084	0.084	0
P_{W2}, MW	0.084	0	0.084	0.084	0
P_{W3}, MW	0.084	0	0.084	0.084	0

Table 5: Pre-determined loads to be shed and amount of f(x) in various load schemes

Load Scheme	Pre-determined loads to be shed	$f(x)$($)
1	L_{1-DR}, L_{2-DR}, L_{3-DR}, L_{6-DR}, L_{7-DR}, L_{8-DR}, L_{9-DR}, L_{10-DR}	1799.407
2	L_{4-DR}, L_{5-DR}, L_{6-DR}, L_{7-DR}, L_{8-DR}, L_{9-DR}, L_{10-DR}	1951.779
3	L_1, L_{1-DR}, L_{3-DR}, L_{4-DR}, L_{5-DR}, L_{6-DR}, L_{7-DR}, L_{8-DR}, L_{9-DR}, L_{10-DR}, L_{11-DR}	3550.510
4	L_1, L_5, L_{1-DR}, L_{3-DR}, L_{4-DR}, L_{5-DR}, L_{6-DR}, L_{7-DR}, L_{8-DR}, L_{9-DR}, L_{10-DR},L_{11-DR}	8013.048
5	L_1, L_2, L_3, L_5, L_{3-DR}, L_{4-DR}, L_{5-DR}, L_{6-DR}, L_{7-DR}, L_{8-DR}, L_{9-DR}, L_{10-DR}, L_{11-DR}	10349.702

Table 6: Proposed UFLS procedure in various load schemes

Load scheme	Power deficit	step	curtailing loads	Pre determined	curtailing loads	Minimum acceptable frequency
		1	L_{1-DR}, L_{2-DR}, L_{7-DR}, L_{9-DR}, L_{10-DR}			
1	2.91	2	L_{8-DR}	1.499	1.1658	48.282
		3	-			
		1	L_{4-DR}, L_{8-DR}, L_{9-DR}			
2	3.16	2	L_{7-DR}, L_{10-DR}	1.6251	1.6251	47.90
		3	L_{5-DR}, L_{6-DR}			
		1	L_{1-DR}, L_{3-DR}, L_{4-DR}, L_{6-DR}, L_{7-DR}, L_{9-DR}			
3	3.5	2	L_1, L_{10-DR}, L_{11-DR}	1.9894	1.9894	47.811
		3	L_{5-DR}, L_{8-DR}			
4	4.12	-	L_1, L_5, L_{1-DR}, L_{3-DR}, L_{4-DR}, L_{5-DR},L_{6-DR}, L_{7-DR}, L_{8-DR}, L_{9-DR}, L_{10-DR}, L_{11-DR}	2.51	2.51	47.904
5	4.37	-	L_1, L_2, L_3, L_5, L_{3-DR}, L_{4-DR}, L_{5-DR}, L_{6-DR}, L_{7-DR}, L_{8-DR}, L_{9-DR}, L_{10-DR}, L_{11-DR}	2.71	2.71	47.51

SFR pattern is not needed. Moreover, the proposed procedure offers a ROCOF based method that factors in load voltage dependence and network critical frequency.

Moreover, this paper illustrates the effect of DR programs in an islanded distribution network. Using DR programs can help DNO shed fewer loads and reduce the amount of the cost function. On the other hand, DR programs impose an excessive unintentional delay time which can be problematic in large power unbalances. To solve the problem, we suggest using suppliers with a big inertia or to limit the use of DR programs and prevent use of them in a large power deficiency. In this paper, this limitation boundary is gained by analyzing system operation in various load schemes in an offline mode. It is obvious that the power deficit that occurred in the fifth load scheme is a boundary limit for use of a DR program in the Danish 14 bus test case. If the severity of the event is bigger than the fifth load scheme, we are not permitted to use DR programs due to the unallowable frequency decrease that may occur, which would cause system blackout.

References

[1] Philip M Anderson and M_ Mirheydar. A low-order system frequency response model. *IEEE Transactions on Power Systems*, 5(3):720–729, 1990.

[2] Pouya Babahajiani, Hassan Bevrani, and Qobad Shafiee. Intelligent coordination of demand response and secondary frequency control in multi-area power systems. In *1st IEEE Conference on New Research Achievements in Electrical and Computer Engineering (CBCONF), Tehran, Iran, May*, 2016.

[3] Pouya Babahajiani, Qobad Shafiee, and Hassan Bevrani. Intelligent demand response contribution in frequency control of multi-area power systems. *IEEE Transactions on Smart Grid*, 2016.

[4] Yu-Qing Bao and Yang Li. Fpga-based design of grid friendly appliance controller. *IEEE transactions on smart grid*, 5(2):924–931, 2014.

[5] Vladimir Chuvychin and Roman Petrichenko. Development of smart underfrequency load shedding system. *Journal of Electrical Engineering*, 64(2):123, 2013.

[6] B Delfino, S Massucco, A Morini, P Scalera, and F Silvestro. Implementation and comparison of different under frequency load-shedding schemes. In *Power Engineering Society Summer Meeting, 2001*, volume 1, pages 307–312. IEEE, 2001.

[7] Amin Gholami, Tohid Shekari, Farrokh Aminifar, and Mohammad Shahidehpour. Microgrid scheduling with uncertainty: The quest for resilience. *IEEE Transactions on Smart Grid*, 7(6):2849–2858, 2016.

[8] D Hazarika and AK Sinha. Method for optimal load shedding in case of generation deficiency in a power system. *International Journal of Electrical Power & Energy Systems*, 20(6):411–420, 1998.

[9] Nick Jenkins. Embedded generation. *Power engineering journal*, 9(3): 145–150, 1995.

[10] M Karimi, P Wall, H Mokhlis, and V Terzija. A new centralized adaptive underfrequency load shedding controller for microgrids based on a distribution state estimator. *IEEE Transactions on Power Delivery*, 32 (1):370–380, 2017.

[11] Aimin Li and Zexiang Cai. A method for frequency dynamics analysis and load shedding assessment based on the trajectory of power system simulation. In *Electric Utility Deregulation and Restructuring and Power Technologies, 2008. DRPT 2008. Third International Conference on*, pages 1335–1339. IEEE, 2008.

[12] Pukar Mahat, Zhe Chen, and Birgitte Bak-Jensen. Underfrequency load shedding for an islanded distribution system with distributed generators. *IEEE Transactions on Power Delivery*, 25(2):911–918, 2010.

[13] Behnam Mohammadi-Ivatloo, A Mokari, H Seyedi, and S Ghasemzadeh. An improved under-frequency load shedding scheme in distribution networks with distributed generation. *Journal of Operation and Automation in Power Engineering*, 2(1):22–31, 2014.

[14] Amin Mokari-Bolhasan, Heresh Seyedi, Behnam Mohammadi-ivatloo, Saeed Abapour, and Saeed Ghasemzadeh. Modified centralized rocof based load shedding scheme in an islanded distribution network. *International Journal of Electrical Power & Energy Systems*, 62:806–815, 2014.

[15] Sara Mullen and Getiria Onsongo. Decentralized agent-based underfrequency load shedding. *Integrated Computer-Aided Engineering*, 17 (4):321–329, 2010.

[16] Lukasz Bartosz Nikonowicz and Jaroslaw Milewski. Virtual power plants-general review: structure, application and optimization. *Journal of Power Technologies*, 92(3):135, 2012.

[17] D Prasetijo, WR Lachs, and D Sutanto. A new load shedding scheme for limiting underfrequency. *IEEE Transactions on Power Systems*, 9 (3):1371–1378, 1994.

[18] CP Reddy, S Chakrabarti, and SC Srivastava. A sensitivity-based method for under-frequency load-shedding. *IEEE Transactions on Power Systems*, 29(2):984–985, 2014.

[19] Urban Rudez and Rafael Mihalic. Analysis of underfrequency load shedding using a frequency gradient. *IEEE transactions on power delivery*, 26(2):565–575, 2011.

[20] Urban Rudez and Rafael Mihalic. Predictive underfrequency load shedding scheme for islanded power systems with renewable generation. *Electric Power Systems Research*, 126:21–28, 2015.

[21] H Seyedi and M Sanaye-Pasand. Design of new load shedding special protection schemes for a double area power system. *American Journal of Applied Sciences*, 6(2):317, 2009.

[22] M Sforna and M Delfanti. Overview of the events and causes of the 2003 italian blackout. In *Power Systems Conference and Exposition, 2006. PSCE'06. 2006 IEEE PES*, pages 301–308. IEEE, 2006.

[23] Tohid Shekari, Farrokh Aminifar, and Majid Sanaye-Pasand. An analytical adaptive load shedding scheme against severe combinational disturbances. *IEEE Transactions on Power Systems*, 31(5):4135–4143, 2016.

[24] Lukas Sigrist, Ignacio Egido, and Luis Rouco. A method for the design of ufls schemes of small isolated power systems. *IEEE Transactions on Power Systems*, 27(2):951–958, 2012.

[25] V Tamilselvan and T Jayabarathi. A hybrid method for optimal load shedding and improving voltage stability. *Ain Shams Engineering Journal*, 7(1):223–232, 2016.

[26] Vladimir V Terzija. Adaptive underfrequency load shedding based on the magnitude of the disturbance estimation. *IEEE Transactions on Power Systems*, 21(3):1260–1266, 2006.

[27] Costas Vournas. Technical summary on the athens and southern greece blackout of july 12, 2004. *National Technical University of Athens*, 2004.

[28] P Wang and R Billinton. Optimum load-shedding technique to reduce the total customer interruption cost in a distribution system. *IEE Proceedings-Generation, Transmission and Distribution*, 147(1):51–56, 2000.

[29] Ding Xu and Adly A Girgis. Optimal load shedding strategy in power systems with distributed generation. In *Power Engineering Society Winter Meeting, 2001. IEEE*, volume 2, pages 788–793. IEEE, 2001.

[30] BAO Yu-Qing, LI Yang, WANG Beibei, HU Minqiang, and CHEN Peipei. Demand response for frequency control of multi-area power system. *Journal of Modern Power Systems and Clean Energy*, 5(1):20–29, 2017.

[31] Alireza Zakariazadeh, Omid Homaee, Shahram Jadid, and Pierluigi Siano. A new approach for real time voltage control using demand response in an automated distribution system. *Applied Energy*, 117: 157–166, 2014.

Nomenclature

Indices

m Index for Generators.

x The vector of decision variable.

t Index for time.

s Load combination scheme.

p The number of possible load combination schemes.

Parameters

f_n Frequency of nth generator.

P_n^G nth generators active power.

Q_n^G nth generators reactive power.

$EENS_s^t$ Expected energy not served in brownout during of t for the sth load combination scheme.

$ROCOF_n$ ROCOF of nth generator.

H_n nth generators inertia constant.

H_C System central inertia constant.

f_C System centralized frequency.

$ROCOF_C$ System centralized ROCOF.

BS_n Breaker Status of nth generator.

P_i^L Active power of load L in ith bus.

Q_i^L Reactive power of load L in ith bus.

Variables

$E(C_{LS,s}^t)$ Expected cost of shedding loads, in brownout during of t, for the sth load combination scheme.

$P_{LS,s}(x)$ Amount of shedding loads for the sth load scheme.

Appendix

Table 7: Excitation system data of CHP units

Parameters	Value
Measurement Delay (s)	0
Filter Delay Time (s)	0.01
Filter Derivative Time Constant (s)	0
Controller Gain (pu)	250
Controller Time Constant (s)	0.01
Exciter Current Compensation Factor (pu)	0
Stabilization Path Gain (pu)	0.01
Stabilization Path Delay Time (s)	1
Controller Minimum Input	-7.5
Controller Minimum Output	-7.5
Controller Maximum Input	9.35
Controller Maximum Output	9.35

Table 8: Governor system data of CHP units

Parameters	Value
Speed Droop (pu)	0.04
Controller Time Constant (s)	0.4
Actuator Time Constant (s)	0.04
Compressor Time Constant (s)	3
Ambient Temperature Load Limit (pu)	0.9
Turbine Factor (pu)	1
Frictional Losses Factor (pu)	0
Turbine Rated Power (MW)	0

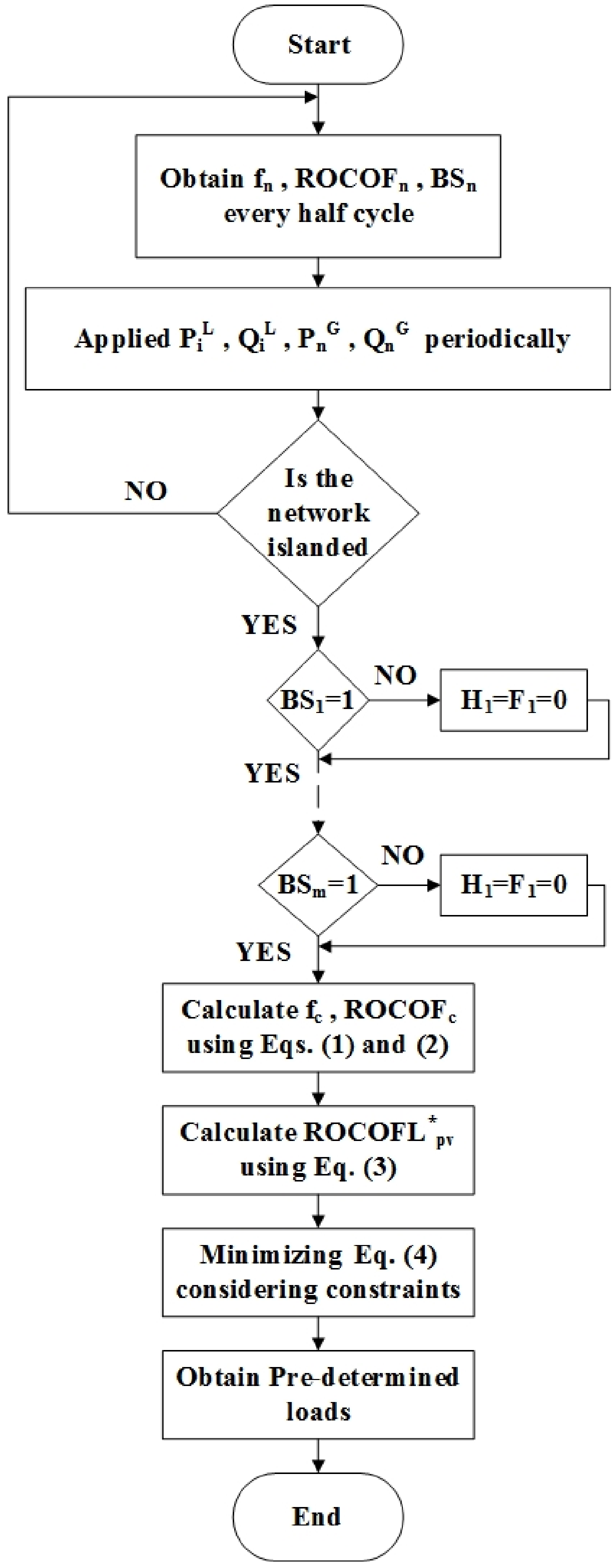

Figure 1: Flowchart of the PLSC module

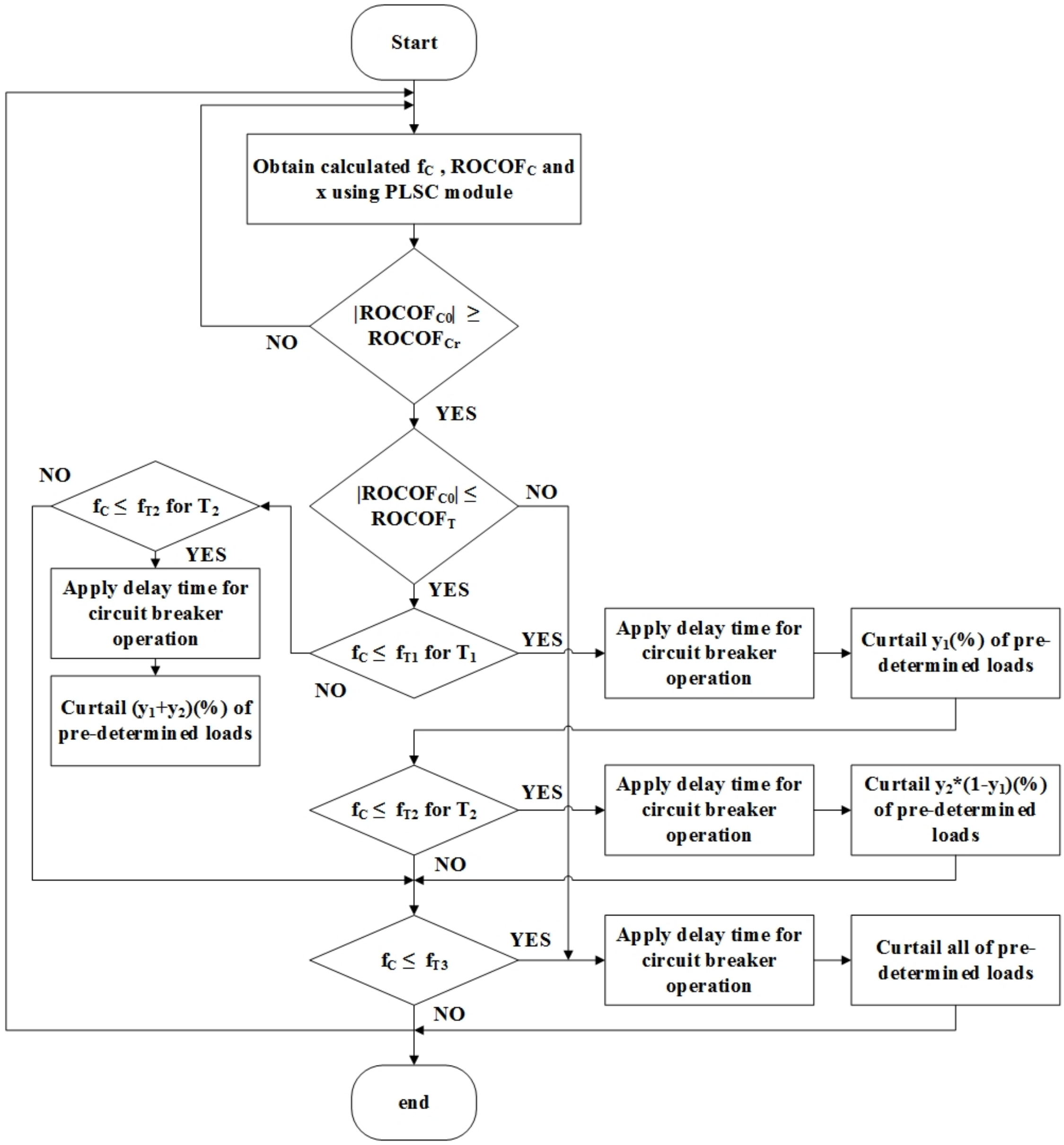

Figure 2: Flowchart of the DLSC module

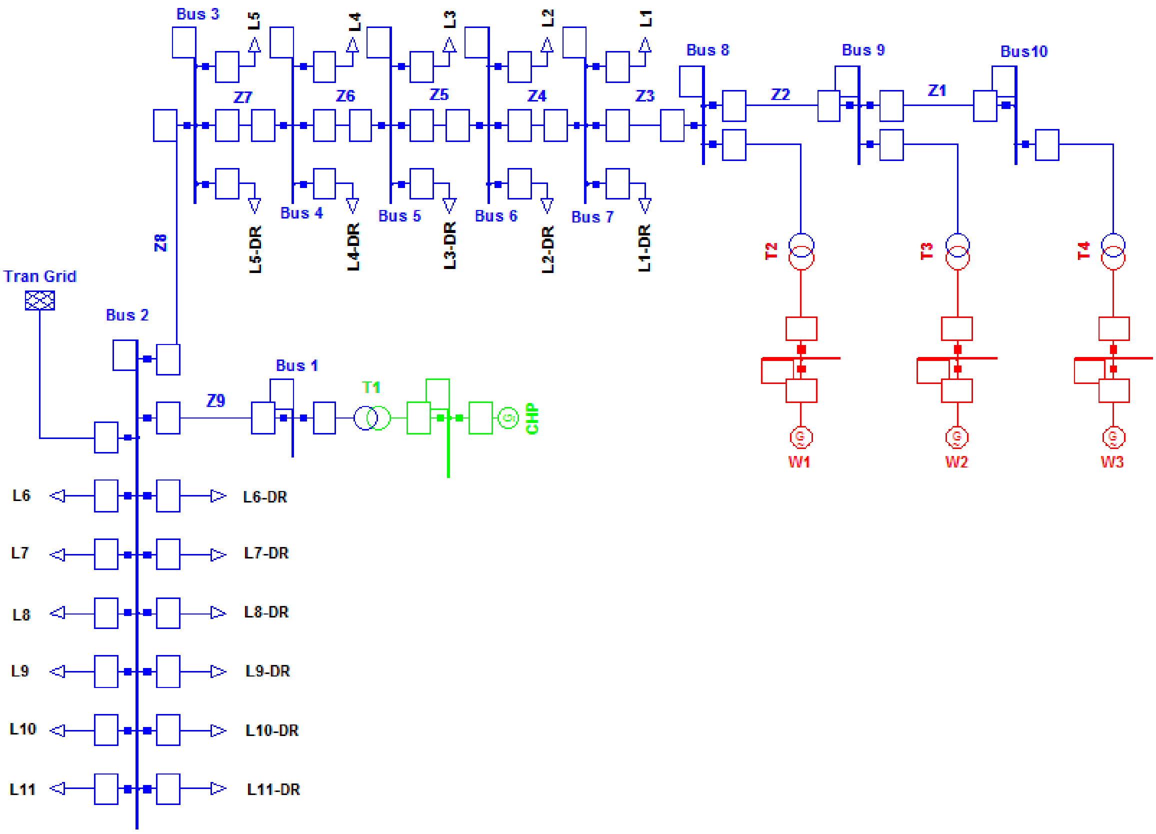

Figure 3: Single line diagram of case study

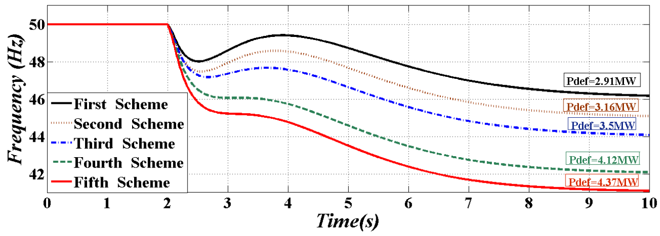

Figure 4: System frequency without implementing of UFLS methods in various load schemes

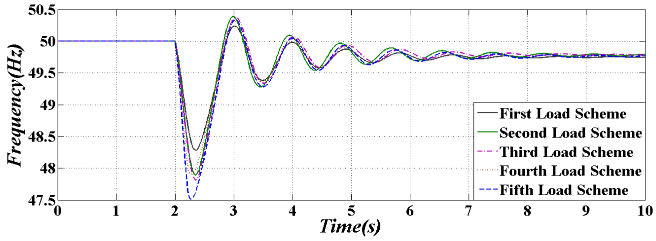

Figure 5: System frequency after using the proposed load shedding method with the DR programs at issue

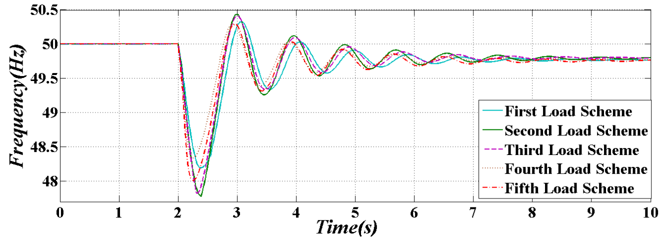

Figure 6: System frequency after using the proposed load shedding method without considering DR programs

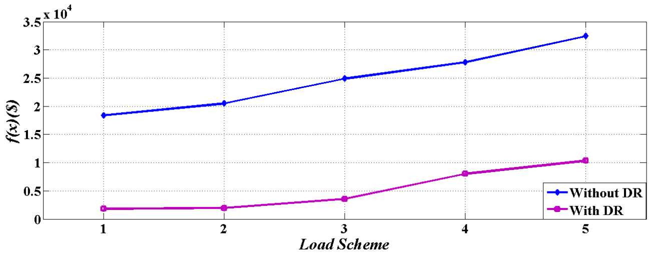

Figure 7: Cost function in two different states of DR programs in five different load shedding schemes

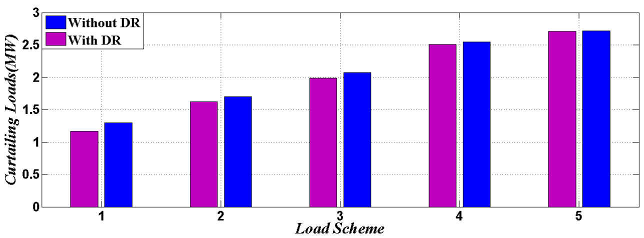

Figure 8: Amount of curtailing loads in two different states of DR programs in five different load shedding schemes